

# Dalton Transactions

Accepted Manuscript



This is an *Accepted Manuscript*, which has been through the Royal Society of Chemistry peer review process and has been accepted for publication.

*Accepted Manuscripts* are published online shortly after acceptance, before technical editing, formatting and proof reading. Using this free service, authors can make their results available to the community, in citable form, before we publish the edited article. We will replace this *Accepted Manuscript* with the edited and formatted *Advance Article* as soon as it is available.

You can find more information about *Accepted Manuscripts* in the [Information for Authors](#).

Please note that technical editing may introduce minor changes to the text and/or graphics, which may alter content. The journal's standard [Terms & Conditions](#) and the [Ethical guidelines](#) still apply. In no event shall the Royal Society of Chemistry be held responsible for any errors or omissions in this *Accepted Manuscript* or any consequences arising from the use of any information it contains.

## ARTICLE

# Theory-Assisted Development of a Robust and Z-Selective Olefin Metathesis Catalyst

Cite this: DOI: 10.1039/x0xx00000x

Giovanni Occhipinti,<sup>a</sup> Vitali Koudriavtsev,<sup>a</sup> Karl W. Törnroos<sup>a</sup> Vidar R. Jensen<sup>\*a</sup>Received 00th January 2012,  
Accepted 00th January 2012

DOI: 10.1039/x0xx00000x

www.rsc.org/

DFT calculations have predicted a new, highly Z-selective ruthenium-based olefin metathesis catalyst that is considerably more robust than the recently reported (SIMes)(Cl)(RS)RuCH(o-OiPrC<sub>6</sub>H<sub>4</sub>) (**3a**, SIMes = 1,3-dimesityl-4,5-dihydroimidazol-2-ylidene, R = 2,4,6-triphenylbenzene) [J. Am. Chem. Soc., 2013, 135, 3331]. Replacing the chloride of **3a** by an isocyanate ligand to give **5a** was predicted to increase the stability of the complex considerably at the same time as moderately improving the Z-selectivity. Compound **5a** is easily prepared in a two-step synthesis starting from Hoveyda-Grubbs second-generation catalyst **3**. In agreement with the calculations, the isocyanate-substituted **5a** appears to be somewhat more Z-selective than the chloride analogue **3a**. More importantly, **5a** can be used in air, with unpurified and non-degassed substrates and solvents, and in the presence of acids. These are traits that are unprecedented among highly Z-selective olefin metathesis catalysts and also very promising with respect to applications of the new catalyst.

## Introduction

Selective synthesis of Z-olefins has for many years been a major goal in olefin metathesis.<sup>1, 2</sup> Only recently, with the discovery of Z-selective molybdenum and tungsten-based catalysts<sup>3-5</sup> followed by ruthenium-based counterparts<sup>6-8</sup> (see Figure 1) has Z-selective synthesis of olefins become an area of application for olefin metathesis.<sup>9-13</sup>

However, all the Z-selective systems reported so far are significantly less robust than the corresponding non-selective catalysts used in commercial processes, such as the Hoveyda-Grubbs second-generation catalyst. To obtain high Z-selectivity combined with high yields and satisfactory TONs using the recently developed catalysts, typically require argon atmosphere, degassed and purified substrates and solvents as well as absence of acid.<sup>3, 4, 7, 8, 14</sup> All this contributes to reducing the scope of Z-selective olefin metathesis and calls for the development of more robust and tolerant catalysts.

One of the new Z-selective catalysts is obtained by simply replacing one of the chloride ligands of the Hoveyda-Grubbs second generation catalyst by 2,4,6-triphenylbenzene thiolate.<sup>8</sup> This catalyst was developed in our group based on DFT calculations predicting that a large aryl thiolate would not only impose the much-wanted selectivity, but the calculated ruthenium–thiolate bond energies were also higher than those of ruthenium–chloride, suggesting that the new and important ligand would remain bound to the metal.<sup>15</sup> In other words, catalyst decomposition via dissociation of the thiolate ligand did not seem likely.

Having synthesized the new catalyst, we were pleased to observe Z-selectivities up to 96 % at low substrate conversion for a range of olefin homocoupling reactions. A very high

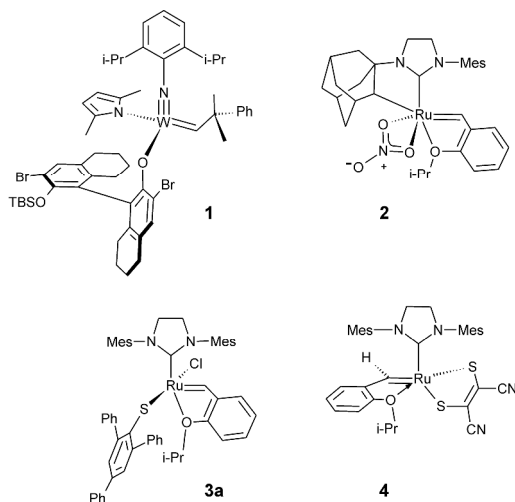


Figure 1 Z-selective catalysts.

kinetic, or “inherent”,<sup>8</sup> selectivity was thus obtained in agreement with the predictions.

However, for most of the substrates tested, a significant amount of isomerization of both starting material and product was observed at high substrate conversion. For example, the metathesis/isomerization ratio recorded in the case of allylbenzene was lower than 1 at low substrate conversion and reached 0.15 at full conversion (> 99%), implying that most of the allylbenzene molecules underwent isomerization rather than metathesis. At the same time isomerization of the metathesis product reduced the *Z*-selectivity from 80–83 % at low substrate conversion to less than 40 % at full conversion (> 99%). These side reactions are presumably promoted by ruthenium–hydride species formed during the catalytic process, as also suggested by the double bond migration which was observed with some substrate.<sup>8, 16–18</sup> Attempts to suppress the isomerization of the substrate by standard additives (e.g. quinones and acids)<sup>17, 19</sup> resulted in reduced *Z*-content of the target product. We also observed that the presence of even traces of acid promoted the formation of Hoveyda-Grubbs second generation catalyst **3**, presumably by anionic exchange<sup>20, 21</sup> The problems with isomerization and progressive formation of the symmetric and unselective **3** during catalysis seriously hamper its use in practical olefin metathesis reactions.

The question thus is whether it is possible to design a more robust and useful variant of **3a**, one that to a lesser extent loses *Z*-selectivity via decomposition to the highly active and unselective **3**. Such a modified catalyst should also be at least as *Z*-selective as **3a** and should be stable enough to tolerate common isomerization-suppressing additives. We recall that, apart from the Ru–SR bond strength, properties relevant for the stability were not part of the initial DFT-based design procedure, which was almost exclusively dedicated to identifying compounds giving high *Z*-selectivity. We now suggest that the main “culprit” responsible for the problems of stability and isomerization could be the remaining chloride in **3a**. In fact, there are several examples of cationic ruthenium complexes formed via dissociation of chloride.<sup>22, 23</sup> Moreover, based on quantum chemical calculations, it has recently been suggested that the Ru–Cl bonds in ruthenium olefin metathesis catalysts such as those of **3** are weak and that dissociation of these ligands may be a competitive side reaction during catalysis.<sup>24</sup> The strong Ru–SR bond and the expected higher trans influence and trans effect of the thiolate ligand compared to that of chloride suggest that the chloride trans to the thiolate in **3a** could be particularly labile.

In this work we thus set out to first test, computationally, the hypothesis as to the weak Ru–Cl bond in **3a**, and then to identify an alternative small monoanionic ligand that would bind more strongly to ruthenium and be less labile. We settled for isocyanate, which is a relatively small (important for maintaining selectivity) and non-toxic pseudohalide. Moreover, isocyanate has already been successfully employed as a ligand in ruthenium-based olefin metathesis catalysts.<sup>25–27</sup> Next, we have followed up this prediction and synthesized and tested, in olefin metathesis experiments, the new isocyanate-substituted

catalyst. Finally, the key step of one of the most probable decomposition reactions of **3a** is investigated by DFT calculations and the mechanistic origin of the improved robustness of the new catalyst is discussed.

## Results and discussion

### Initial computational exploration

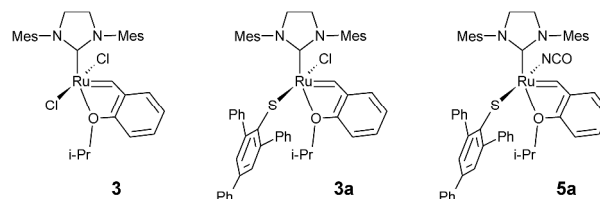


Figure 2 Existing (**3** and **3a**) and predicted (**5a**) catalysts.

The lability of a ligand is determined by its barrier to dissociation. However, the corresponding transition states of weakly bound moieties are often hard to locate,<sup>28</sup> and in many cases an enthalpic barrier arising from a transition state on the potential energy surface (PES) does not even exist. Several scans of the PES of chloride dissociation from **3** and **3a** were carried out, leading to monotonically rising energy with increasing Ru–Cl distance and no indication of a transition state. Of course, a barrier could still exist on the free energy surface, arising in part from solvation and entropy effects,<sup>28, 29</sup> but the determination of such barriers is not necessary for the present more qualitative purpose of identifying a covalent ligand that would be more strongly bound to ruthenium. In fact, the increasing electronic energy calculated as a function of Ru–Cl distance strongly suggest a “very late transition state” and that, in the spirit of Hammond,<sup>30</sup> it would make sense to use the dissociated state in the a qualitative comparison of the lability of Ru–Cl and Ru–NCO bonds.

We first calculated the bond dissociation energy (BDE) of Ru–Cl and Ru–NCO bonds in **3a** and **5a** respectively; see Table 1. These results were then compared with the corresponding calculated BDE of the Ru–Cl bond in the Hoveyda-Grubbs second-generation catalyst **3**. Dissociation of the chloride ligand from complex **3a** in THF solution (the solvent used in the present experiments) requires 12 kcal/mol, which is half the energy required to dissociate the same ligand from catalyst **3**. This result confirms our above-mentioned concern with respect to the lability of the chloride ligand. On the other hand, the dissociation of isocyanate from **5a** is more energy demanding (21 kcal/mol). Thus, the lability of isocyanate in **5a** is predicted to be comparable to that of chloride in **3**, which is among the most robust and successful olefin metathesis catalysts.

Table 1 Ru–X bond dissociation energies in solution<sup>a</sup>

entry	X	complex	$\Delta G_{\text{THF}}^c$	$\Delta G_{\text{DCM}}^d$
1	Cl	<b>3</b>	24.7	22.6
2	Cl	<b>3a</b>	12.4	10.2
3	SAI <sup>b</sup>	<b>3a</b>	29.3	28.0
4	NCO	<b>5a</b>	21.1	19.2
5	SAI <sup>b</sup>	<b>5a</b>	29.2	27.7

<sup>a</sup>Energies in kcal/mol. <sup>b</sup>2,4,6-triphenylbenzenethiolate. <sup>c</sup>Tetrahydrofuran.

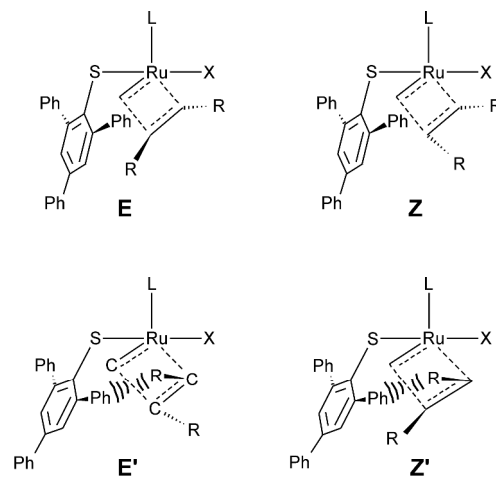
<sup>d</sup>Dichloromethane.

Next, we evaluated the effect of replacing chloride with isocyanate on the Z-selectivity in homocoupling of allylbenzene as promoted by **3a** and **5a**. Scheme 1 shows the most favourable pathway for formation of E- and Z-olefin, respectively. The other two pathways (denoted E' and Z' in Figure 3) are energetically less favoured because they require the formation of more crowded minima and saddle points<sup>15</sup> in which one of the R substituents on the olefin is pointing towards one of the *ortho*-substituents of the thiolate ligand.

The selective formation of E- and Z-olefins using ruthenium-based catalysts has recently been the focus of several computational contributions<sup>15, 31-34</sup> in which both non-selective and Z-selective catalysts have been investigated. In general it has been found that the rupture of the metallacyclobutane is energetically more demanding than its formation. For the Z-selective catalysts, including the ruthenium thiolate-based catalysts,<sup>15</sup> the transition state leading to the rupture of the metallacyclobutane represents the highest barrier of the reaction. In other words, to evaluate the Z-selectivity of a catalyst it suffices to calculate only the relative free energies of this stationary point, termed TS2 in Scheme 1.

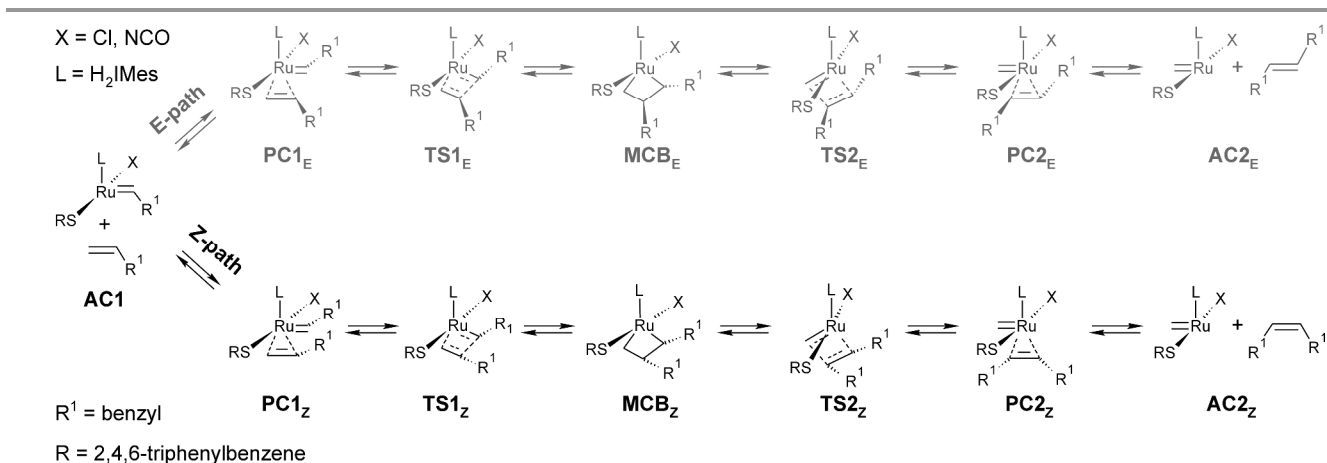
Table 2 shows the relative energies of TS2 for the E- and Z-pathways as obtained for **3**, **3a** and **5a**. In agreement with experiments, the calculated Gibbs free energy measure of Z-selectivity,  $\Delta G_{\text{THF}} = G_{\text{THF}}(\text{E}) - G_{\text{THF}}(\text{Z})$  at 298 K in THF solution is negative for **3** (– 1.0 kcal/mol), which indicates that

the formation of the E-isomer is kinetically preferred over the Z-isomer, while it is positive for both **3a** and **5a**. In particular, it is larger for **5a** than for **3a**, suggesting that homocoupling of allylbenzene should be more Z-selective with **5a** than with **3a**. In other words, replacement of chloride ligand with isocyanate should be beneficial for the Z-selectivity. However, as the Z-selectivity is dependent on the nature of the substrate, and also on the catalyst-substrate combination, this prediction cannot automatically be extended to any possible transformation and substrate.



**Stability: E > E' and Z > Z'**

Figure 3. Relative stability of the four stereoisomers of the transition state for rupture of the metallacyclobutane (MCB) intermediate, TS2. See Scheme 1 for the pathways leading to formation of E- and Z-olefins.



Scheme 1: Reaction pathway for metathesis of allylbenzene using **3a** and **5a**, leading to corresponding (E)- (via the E-path) and (Z)-1,4-diphenyl-2-butene (via the Z-path) products.

## ARTICLE

Table 2 Relative energies (kcal/mol) of TS2 for MCB rupture following E and Z pathways<sup>a</sup>

entry	complex	$\Delta E_{\text{gas}}$	$\Delta G_{\text{gas}}$	$\Delta G_{\text{THF}}$
1	<b>3</b>	-0.7	-0.8	-1.0
2	<b>3a</b>	3.4	2.7	1.0
3	<b>5a</b>	3.7	4.2	2.2

<sup>a</sup> The relative energies are a measure of Z-selectivity,  $\Delta G_{\text{THF}} = G_{\text{THF}}(\text{E}) - G_{\text{THF}}(\text{Z})$ .

## Experimental follow up of prediction

Encouraged by the above computational results we decided to synthesize ruthenium complex **5a**. Complex **5a** was prepared in high yield (92 %) by reacting the bis-isocyanate complex **5**, with potassium 2,4,6-triphenylbenzenethiolate, see Scheme 2. The bis-isocyanate complex **5** was prepared in a single step according to a literature procedure based on reacting the commercially available Hoveyda-Grubbs second-generation catalyst **3** with silver cyanate.<sup>26</sup> Crystals suitable for X-ray-diffraction analysis were grown by slow diffusion of pentane into a concentrated solution of **5a** in dichloromethane at  $-32^\circ\text{C}$ . Figure 4 shows the corresponding X-ray structure of **5a**. The isocyanate ligand is nearly linear (Ru1-N1-C35 =  $169^\circ$ ).

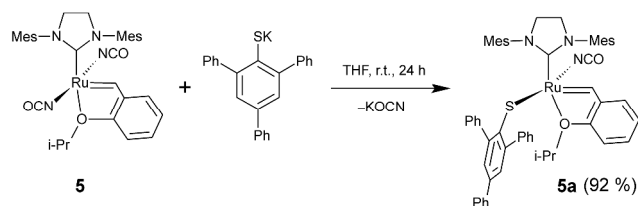
Scheme 2 Preparation of complex **5a**.

Table 3 Metathesis homocoupling of terminal olefins under argon atmosphere

entry	substrate	catalyst	cat. loading mol %	solvent (M)	temp., $^\circ\text{C}$	time, h	% conv. <sup>b</sup>	yield <sup>b</sup> (isolated) <sup>c</sup>	% Z <sup>b</sup>
1	allyl trimethylsilane	<b>3a</b> <sup>a</sup>	0.25	THF (4)	60	18	22	12 (11)	95
2	allyl trimethylsilane	<b>5a</b> <sup>a</sup>	0.25	THF (4)	60	16	14	9 (6)	96
3	allylbenzene	<b>3a</b>	0.25	THF (4)	40	0.5	38	12	80
4	allylbenzene	<b>5a</b>	0.25	THF (4)	40	0.5	20	6	88
						2	> 99	10	56
5	1-octene	<b>3a</b>	0.01	neat	60	2	24	20 (15)	86
6	1-octene	<b>5a</b>	0.01	neat	60	1.5	20	13 (10)	88

<sup>a</sup> Additive: 1,8-bis(dimethylamino)naphthalene (0.12 mol%). <sup>b</sup> Determined by  $^1\text{H}$  NMR. <sup>c</sup> Isolated yield.

Complex **5a** was initially tested under argon atmosphere as a Z-selective catalyst for homocoupling metathesis of terminal olefins. Table 3 compares the catalytic properties of **5a** with

those of **3a**.<sup>8</sup> The catalytic tests give rather similar results for the two catalysts, although **5a** appears to be slightly more Z-selective and less active than **3a** in general. The tendency to

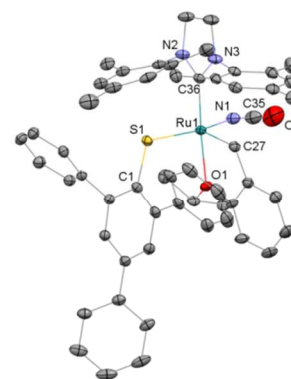


Figure 4. ORTEP-style diagram of **5a** with the displacement ellipsoids drawn at the 50 % probability level. Hydrogen atoms and the solvent molecule (dichloromethane) have been omitted for clarity. Selected geometrical parameters: Ru1–C27 = 1.834(2) Å, Ru1–C36 = 1.991(2) Å, Ru1–S1 = 2.3091(6) Å, Ru1–O1 = 2.2272(17) Å, Ru1–N1 = 2.049(2) Å, Ru1–S1–C1 = 110.03(8)°, N1–Ru1–S1 = 155.92(7)°, Ru1–N1–C35 = 169.1(2)°

isomerization of the substrate (terminal olefin  $\rightarrow$  internal olefin) and of the product (Z  $\rightarrow$  E isomerization) is also similar. These side reactions are substrate-dependent and their rate increases rapidly with substrate conversion.<sup>8</sup> For example, entries 3 and 4 show that, despite the conversion of allylbenzene being almost complete after two hours with both catalysts, the yield of the target product practically does not increase after the first half an hour. In contrast, the Z-content of the target product drops radically after the first 30 minutes.

As a sign of a more notable difference between the two catalysts, we observed that complex **5a** is stable on silica gel and could be purified by column chromatography using unpurified solvents. Complex **3a**, on the other hand, decomposes under the same conditions. In order to assess the relative robustness of the two complexes, we monitored their decomposition in CD<sub>2</sub>Cl<sub>2</sub> solution at room temperature using <sup>1</sup>H NMR; see the Supplementary Information for details. Whereas after 20 hours in the presence of air, **3a** is completely decomposed, **5a** still largely remains intact (87 %). Even after two weeks there is still a considerable fraction of **5a** (21 %) present in solution.

Complex **5a** also tolerates acids well. For example, when dissolved in CD<sub>2</sub>Cl<sub>2</sub> in the presence of one equivalent of phenylphosphoric acid and in argon atmosphere, only a small amount (2%) is decomposed after 20 hours. In comparison, one

third of **3a** is decomposed under the same conditions; see the Supplementary Information for further details.

These results prompted us to investigate the catalytic properties of **5a** in air, using non-degassed and unpurified substrate and solvent. Table 4 shows the homocoupling of seven different terminal olefins conducted in air under various reaction conditions. Entries 1 and 2 compare the performance of catalysts **3a** and **5a** in the homocoupling of neat allylbenzene performed at room temperature using low catalyst loading (0.1 mol %). After three hours only a tiny amount (about 2 %) of the product is recorded with both catalysts. However, whereas the Z-selectivity with **5a** (86 %) is high and similar to that observed in argon atmosphere (for example, entry 4, see Table 3), the product achieved with **3a** only has a moderate Z-content (46 %).

After 21 hours the Z-content obtained using **3a** is significantly reduced (21 %) and essentially comparable to that observed with a non-selective catalyst (e.g. Hoveyda-Grubbs second generation). In contrast, using **5a** the Z-selectivity remains high and almost matches that (83 %) recorded after three hours (86 %). In other words, the Z–E isomerization of the target product is significantly slower in air than in argon (cf., entry 4, Table 3, and entry 2, Table 4). Moreover, we were pleased to note that the presence of air to a large extent also suppresses isomerization of the starting material (the substrate).

Table 4 Metathesis homocoupling of terminal olefins in air

entry	substrate	catalyst	cat. loading mol %	solvent (M)	temp., °C	time, h	% conv. <sup>a</sup>	yield <sup>a</sup> (isolated) <sup>b</sup>	% Z <sup>a</sup>
1	allylbenzene	<b>3a</b>	0.1	neat	20	3	2.5	2.2	46
						21	18	17.5	21
2	allylbenzene	<b>5a</b>	0.1	neat	20	3	2	2	86
						21	15.5	15 (15)	83
3	allylbenzene	<b>5a</b>	1	neat	20	18	44	41	83
						52	58	53 (52)	80
4	phenylbutene	<b>5a</b>	1	neat	20	18	48	48	86
						36	61	61	83
						61	69	69 (67)	79
5	methyl undecenoate	<b>5a</b>	1	neat	35	15	21	19	75
						12	5	5 (5)	91
6	<i>N</i> -allylanyliline	<b>5a</b>	1	neat	35	12	5	5 (5)	91
						6	44	39	81
7	1-hexene	<b>5a</b>	1	THF (4)	35	22	55	48 (20)	75
						2	32	28	83
8	1-octene	<b>5a</b>	1	THF (4)	35	6	50	45	75
						22	73	64 (44)	67
						3	6.5	6	74
9	2-(alloy)-ethanol	<b>5a</b>	1	THF (4)	35	10	41	8	65

<sup>a</sup>Determined by <sup>1</sup>H NMR. <sup>b</sup>Isolated yield.

Presumably, formation of Ru–hydride complexes, generally believed to be the main responsible for isomerization processes with Ru-based catalysts,<sup>16–18, 35–37</sup> is more difficult in air than under argon atmosphere. This, together with the expected lower stability of such hydrides in air compared to that of **5a**, presumably explains the better results of **5a** in air compared to those of **3a**. In order to achieve higher yields, we repeated the same reaction using higher catalyst loading (1 mol %) and longer reaction time (entry 3). After 52 hours, the conversion of

the starting material reached 58 %, and the product was isolated in 52 % yield combined with a Z-selectivity of 80 %.

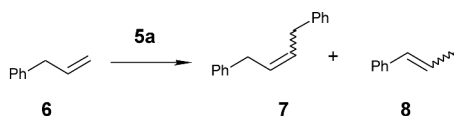
Entry 4 shows the homocoupling of phenylbutene carried out under the same conditions as entry 3. After 61 hours, the product was obtained in 69 % yield and a Z-content of 79 %. Interestingly, no isomerization of the starting material was observed with this substrate.

For less reactive substrates, such as methyl undecenoate and *N*-allylanyliline, entries 5 and 6 respectively, the reaction was

performed at 35 °C rather than at room temperature. Gratifyingly, even under these conditions olefin metathesis proceeds with high Z-selectivity. The two target products were again achieved with a high Z-content, although the yields were rather low. Also in this case only little or no isomerization of the starting materials was observed. Finally, due to the low solubility of the catalyst in the neat substrate, homocoupling of 1-hexene, 1-octene, and 2-(aloxo)-ethanol were carried out in THF solution at 35 °C. Again, the products were achieved with high Z-selectivity. In the case of 1-hexene and 1-octene, a Z-selectivity of 81 % and 75 % combined with a yield of 39 % and 45 % respectively was recorded after six hours. Higher yields, 48 % and 64 % respectively, with a somewhat lower Z-selectivity (75 % and 69 %) could be achieved after 22 hours. With these two substrates, the isomerization of the starting material was slow and the ratio metathesis/isomerization decreased only slightly with the substrate conversion.

After three hours, the product of 2-(aloxo)-ethanol was achieved in a yield of 6 % and a Z-selectivity of 74 %, and again with only little isomerization of the starting material. Unfortunately, by prolonging the reaction time the amount of isomerization increased significantly. After 10 hours, the conversion of the substrate was 40 %, but the yield (8 %) was only slightly higher than that recorded after three hours.

Overall, the experiments in Table 4 demonstrate that complex **5a** is able to promote the homocoupling of different substrates in air with high Z-selectivity. This suggests that, not only the precursor **5a**, but also the reaction intermediates (cf., Scheme 1) of the catalytic process are relatively stable in air.



Scheme 3 Metathesis homocoupling of allylbenzene

Table 5 Allylbenzene homocoupling with **5a** in air (in solution), after 4 hours<sup>a</sup>

entry	solvent	% conv. <sup>b</sup>	7/8 <sup>b</sup>	% Z <sup>b</sup>
1	ethyl acetate	27	5.8	79
2	methyl acetate	16	9.3	81
3	tetrahydrofuran	13	6.9	86
4	dioxane	15	3.8	85
5	methanol	14	2	86
6	ethanol	11	14.3	81
7	isopropanol	20	2.4	84
8	acetone	9	4.3	75
9	toluene	17	16	69
10	fluorobenzene	23	6.7	58
11	dichloromethane	17	7.5	64

<sup>a</sup> Reaction conditions: catalyst loading 0.25 mol%, allylbenzene 2 mmol, Substrate concentration 4M, T = 40 °C; Time, 4 hours. <sup>b</sup> Determined by <sup>1</sup>H NMR.

In order to identify the best reaction conditions metathesis of allylbenzene was performed in different non-degassed and unpurified solvents, at different temperatures and at different substrate concentrations; see Tables 5, 6, and 7. Despite the

presence of air and a temperature of 40 °C, none of the tested solvents were truly unsuitable for this reaction and Z-selectivities in the range 58–86 % were recorded, see Table 5. The Z-selectivity is high (81–86 %) even in protic solvents such as methanol, ethanol, and isopropanol. In addition, with ethanol the selectivity for **7** also high (with a 7/8 ratio of 14.3), and ethanol thus is among the best solvents tested for this reaction.

In general, the catalytic outcome (i.e., conversion, metathesis/isomerization, and Z-selectivity) is considerably affected by the solvent, and none of the tested solvents appears to be clearly superior. Whereas the highest conversion (27 %) was obtained with ethyl acetate, the highest ratio metathesis/isomerization (16) was reached in toluene. The highest Z-selectivity (86 %) was obtained in THF and in methanol. Despite the fact that none of the solvents was clearly superior in general, tetrahydrofuran is seen to promote high Z-selectivity with a high metathesis/isomerization (6.9) ratio, and this solvent was thus selected for the screening of temperature (Table 6) and substrate concentration (Table 7).

Table 6. Allylbenzene homocoupling with **5a** at different temperatures<sup>a</sup>

entry	Temperature	time, h	% conv. <sup>b</sup>	7/8 <sup>b</sup>	% Z <sup>b</sup>
1	30	2	16	5.9	87
		4	26	5.9	85
2	40	2	35	2.7	84
		4	48	2.6	78
3	50	2	57	1.4	73
		4	65	1.3	67

<sup>a</sup> Reaction conditions: catalyst loading, 1 mol%; solvent, tetrahydrofuran; substrate concentration, 4M. <sup>b</sup> Determined by <sup>1</sup>H NMR.

Table 6 shows the results of homocoupling of allylbenzene in THF (4M) using 1 mol % of catalyst load at different temperatures. As expected both the conversion of the substrate and the isomerization of the substrate increase significantly with the temperature. For example, after four hours the conversion is 26 % with a metathesis/isomerization ratio of 5.9 at 30 °C, while at 50 °C the conversion is 65 % and the metathesis/isomerization ratio is only 1.3. The Z-selectivity decreases with temperature as well. However, as the Z-selectivity also decreases with substrate conversion, it is very difficult to separate the effects of the temperature from those arising from degree of substrate conversion.

Table 7. Allylbenzene homocoupling with **5a** at different substrate concentrations in THF solution at 40 °C<sup>a</sup>

entry	Sub. Conc., M	time, h	% conv. <sup>b</sup>	7/8 <sup>b</sup>	% Z <sup>b</sup>
1	4	2	8	7	86
		4	13	6.9	86
2	2	2	6	2.4	87
		4	10	2.3	87
3	1	2	3	1.3	89
		4	5	1.3	85

<sup>a</sup> Reaction conditions: catalyst concentration, 0.01 M; solvent, tetrahydrofuran. <sup>b</sup> Determined by <sup>1</sup>H NMR (CDCl<sub>3</sub>).

With the goal to evaluate the effect of dilution on metathesis, we performed some experiments in THF at three different substrate concentrations, keeping the concentration of catalyst constant at 0.01 M; see Table 7. The conversion of the substrate and the selectivity for **7** decrease with the substrate dilution. On

the other hand, the Z-selectivity of the target product seems to be relatively little affected by the substrate concentration. After two hours, substrate dilution seems to lead to slightly increased Z-selectivity. This trend may be a consequence of the fact that the substrate conversion is also lower at higher dilution.

Table 8. Metathesis homocoupling of terminal olefins (neat substrate) in presence of phenylphosphoric acid at room temperature and under argon atmosphere

entry	substrate	catalyst	cat. loading mol %	time, h	% conv. <sup>a</sup>	yield <sup>d</sup> (isolated) <sup>b</sup>	% Z <sup>a</sup>
1	allylbenzene	<b>3a</b>	0.1	3	16	16	18
2	allylbenzene	<b>5a</b>	0.1	2	7	6	86
				16	59	29	80
3	allylbenzene	<b>5a</b>	1	4	46	42	74
				8	68	57 (57)	71
4	methyl undecenoate	<b>5a</b>	0.1	24	7	6.5	83
				48	8.5	8	82
5	methyl undecenoate	<b>5a</b>	1	21	42	37	75
				68	69	61	75

<sup>a</sup> Determined by <sup>1</sup>H NMR. <sup>b</sup> Isolated yield.

As discussed above, complex **5a** tolerates relatively well the presence of small amounts of acid. Phenylphosphoric acid has previously been proposed to be an efficient additive for suppressing olefin isomerization in ruthenium-catalysed metathesis reactions.<sup>19</sup> Table 8 shows the results of metathesis homocoupling of neat allylbenzene and methyl undecenoate in the presence of one equivalent of phenyl phosphoric acid with respect to the catalyst loading. The reactions were carried out at room temperature and under argon atmosphere. Entries 1 and 2 compare the performance of catalysts **3a** and **5a**, respectively, for the homocoupling of allylbenzene using a catalyst loading of 0.1 mol %.

Catalyst **3a** (entry 1) is clearly not Z-selective under these conditions. After three hours, 16 % of the allylbenzene is converted into the target product with a Z-selectivity of only 18 %. In contrast, the recorded Z-selectivity for catalyst **5a** is high (e.g., 86 % with a conversion of 7 % after two hours), which is comparable to those recorded at low substrate conversion either in absence of acid (entry 4, Table 3) or in presence of air (entry 2, Table 4).

The addition of acid appears to speed up the reaction (c.f., entries 2 and 3, Table 4, and entries 2 and 3, Table 8), but air, at least for this substrate, seems to be more efficient than acid in suppressing isomerization of both substrate and product. Such conditions are even more efficient for methyl undecenoate, for which a yield of 61 % could be achieved after 68 hours at room temperature, with a Z-selectivity of 75 %.

### Computational investigation of the anionic exchange decomposition pathway

Hoveyda-Grubbs type catalysts bearing mixed anionic ligands are known to undergo intermolecular anionic ligand exchange under mild conditions in solution,<sup>20</sup> and a reaction mechanism involving the formation of a bridged dimer has been proposed, see Scheme 4. Dimers similar to those proposed as the reaction intermediate **II** (Scheme 4), have been isolated and characterized using X-ray diffraction analysis.<sup>38, 39</sup> This phenomenon explains why stable ruthenium-alkylidene

catalysts bearing small, mixed monodentate anionic ligands are unknown. However, when at least one of the ligands becomes sufficiently big, stable complexes with mixed anionic ligands can be isolated and characterized.<sup>40-42</sup>

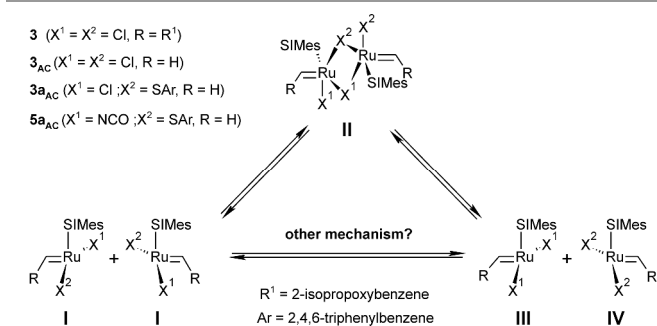
Compounds **3a** and **5a**, which contain one sterically demanding thiolate and a small, anionic ligand are also examples of such compounds. These compounds are stable in solution (e.g., in tetrahydrofuran) even at elevated temperatures (60 °C). However, when **3a** and one equivalent of phenylphosphoric acid are dissolved in CD<sub>2</sub>Cl<sub>2</sub>, Hoveyda-Grubbs second generation catalyst **3** is formed relatively fast. For example, after 20 hours and at room temperature, 16 % of **3** has been formed, see the Supplementary Information for details. In comparison, only a tiny amount (0.5 %) of **5** is formed from **5a** under the same conditions. Formation of **3** and **5** is also observed when a solution of **3a** and **5a** in CD<sub>2</sub>Cl<sub>2</sub> is exposed to air and also in this case **3** is formed much faster.

Formation of the symmetric complexes **3** and **5** (i.e., the symmetric complex **III** in Scheme 4) from the mixed complexes **3a** and **5a** could be explained by an anionic exchange pathway (see Scheme 4). This pathway also produces an equivalent of the bis-thiolate complex (**IV**), which was not observed.† The lack of the bis-thiolate complex (**IV**), could be due to the low stability of this compound in air or in presence of an acid.

In order to shed light on the hypothesis that the symmetric compounds **3** and **5** are generated from **3a** and **5a** via the anionic exchange mechanism depicted in Scheme 4, we decided to investigate this possibility computationally.

We have calculated the Gibbs Free energies in solution of the stationary points **I–IV** for four different tetracoordinate 14 electron ruthenium alkylidenes. Whereas complex **3** is the Hoveyda-Grubbs second generation catalyst with the otherwise chelating 2-isopropoxy moiety of the alkylidene not being coordinated to the ruthenium, **3<sub>AC</sub>** is the corresponding methylidene complex. In order for the computations to be tractable, for the complexes **3a** and **5a**, only the methylidene

versions (i.e., **3a<sub>AC</sub>** and **5a<sub>AC</sub>**), have been considered, see Scheme 4.



Scheme 4 Investigation of the anionic exchange decomposition mechanism for the mono-thiolate complexes

Table 9 shows that the Gibbs free energy of dimer **II** for **3** in dichloromethane is 8.3 kcal/mol higher than that of the monomer **I**. This energy can be regarded as the lower limit of the true barrier (not investigated in the present work) of the anionic exchange reaction. The relative stability of **II** increases dramatically for the methylidene complex **3<sub>AC</sub>** (−11.8 kcal/mol). This stability strongly suggests that **II** may be a potential resting state, or thermodynamic sink, of the Hoveyda-Grubbs second generation catalyst during catalysis.

The importance of this species in catalysis and its potential role as a resting state would be an interesting topic for a future study. Despite the fact that the methylidene dimer has so far never been observed, two structurally closely related dimers, differing from the dimer of **3<sub>AC</sub>** only by the nature of the alkylidene ligand (i.e., fluoromethylidene and chloromethylidene instead of methylidene) have been isolated and characterized.<sup>39</sup>

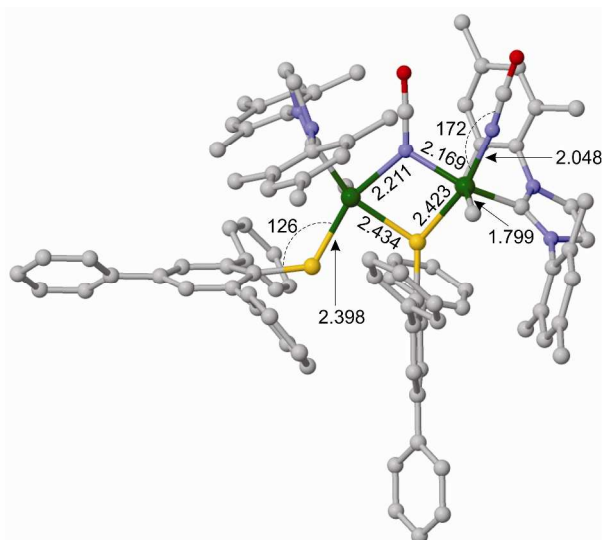


Figure 5. Optimized geometry of the dimer **II** of **5a<sub>AC</sub>**: distances in angstroms and angles in degrees. Hydrogen atoms have been omitted for clarity. Colour coding: C, grey; N, blue; O, red; S, yellow; Ru, green.

For the corresponding thiolate complexes **3a<sub>AC</sub>** and **5a<sub>AC</sub>**, the anionic exchange reaction is predicted to be endergonic (by 5.2 and 3.7 kcal/mol, respectively). Moreover, the dimer **II**, is disfavoured by 18.2 (**3a<sub>AC</sub>**) and 20.4 kcal/mol (**5a<sub>AC</sub>**).

If we assume that the influence of the alkylidene (i.e., the difference between **3** and **3<sub>AC</sub>**) on the stability of **II** is similar among the complexes **3**, **3a**, and **5a**, the estimated relative free energy of **II** for the two latter complexes should be well above 35 kcal/mol. Keeping in mind that **II** is the lower limit of the actual barrier, the anionic exchange mechanism appears unlikely for **3a** and **5a**. Nevertheless, this mechanism cannot be ruled out for smaller reaction intermediates such as **3a<sub>AC</sub>** and **5a<sub>AC</sub>**.

Table 9. Gibbs free energy of the anionic exchange in solution<sup>a</sup>

entry	complex	$\Delta G(\text{I+I})$	$\Delta G(\text{II})$	$\Delta G(\text{III+IV})$
1	<b>3</b>	0	8.3 (8.1)	0
2	<b>3<sub>AC</sub></b>	0	-11.8 (−12.0)	0
3	<b>3a<sub>AC</sub></b>	0	18.2 (18.3)	5.2 (5.9)
4	<b>5a<sub>AC</sub></b>	0	20.4 (20.7)	3.7 (4.6)

<sup>a</sup>Energies in kcal/mol. Relative free energies are for dichloromethane solution, with those of tetrahydrofuran solution in parenthesis.

In fact, as seen from Table 1, dissociation of a chloride ligand from **3a** (10.2 kcal/mol, in CH<sub>2</sub>Cl<sub>2</sub>) and an isocyanate ligand from **5a** (19.2 kcal/mol, in CH<sub>2</sub>Cl<sub>2</sub>) both require less energy than the formation of **II**. Thus, an alternative mechanism for the formation of **3** and **5** could initiate with the dissociation of chloride or isocyanate. The dissociated ligand could then react with another ruthenium complex via an associative mechanism, replacing the thiolate ligand. The presence of a proton source (acid) could promote the dissociation of both the chloride (first step) and the thiolate (second step), thus lowering the corresponding barriers.<sup>††</sup> Due to the fact that the NMR experiments were conducted in presence of an acid or air, the recombination of the dissociated thiolate (from the second step) with the cationic ruthenium-thiolate complex (from the first step) is unlikely to occur before the decomposition of the cationic complex takes place. This could explain why the corresponding bis-thiolate complex is not detected in the <sup>1</sup>H NMR experiments, as described in the Supplementary Information.

The fact that the observed relative rates with which the thiolate complexes decompose correlate with the calculated lability of the anionic ligands (i.e., **3a** > **5a**) suggests that ligand dissociation (first step) could be involved in the rate determining step of the decomposition reaction.

The computational and experimental data combined suggest that the anionic exchange mechanism, which involves a bridged dimer, is unlikely for the large thiolate complexes **3a** and **5a**. The decomposition of these complexes in presence of air or an acid to give **3** and **5**, might instead involve the dissociation of the small anionic ligand (chloride or isocyanate, first step), followed, in a second step, by substitution of the thiolate ligand of another ruthenium complex by the dissociated small ligand of the first step.

## Conclusions

In conclusion, a robust and highly Z-selective olefin metathesis catalyst has been developed with the assistance of DFT calculations. The new catalyst is prepared in a two-step synthesis starting from Hoveyda-Grubbs second-generation catalyst **3**. The two chloride ligands of **3** are replaced by 2,4,6-triphenylbenzene thiolate and isocyanate, respectively. DFT calculations suggest that the origin of the robustness is related to the stronger ruthenium–isocyanate than ruthenium–chloride bonds in these complexes. They also suggest that the size of the thiolate ligand prevents anionic exchange via dimer formation, otherwise a common decomposition mechanism for Hoveyda-Grubbs alkylidenes. The novel catalyst can be used in air, with unpurified and non-degassed substrates and solvents, and in the presence of acids.

## Computational Details

### Geometry optimizations.

All geometry optimizations were performed using the hybrid range-separated functional including empirical atom–atom dispersion,  $\omega$ B97XD, as implemented in Gaussian 09.<sup>43</sup> The  $\omega$ B97XD<sup>44–46</sup> functional was chosen due to its excellent performance in reproducing X-ray geometries of ruthenium-based olefin metathesis catalysts and other functional transition metal compounds.<sup>47</sup> Input geometries were constructed using the Spartan software package<sup>48</sup> by modifying the available X-ray structures<sup>49</sup> or previously DFT-D geometry optimized geometries. When available (**3**,<sup>50</sup> **3a**,<sup>8</sup> and **5a**), the X-ray structures from Cambridge Structural Database (CSD)<sup>49</sup> were used as starting points for geometry optimizations. Conformational searches were performed routinely at the MMFF<sup>51</sup> force-field level using Spartan software package.<sup>48</sup>

Numerical integrations were performed using the default “ultrafine” grid of Gaussian 09. Default values were adopted for self-consistent-field (SCF) convergence criteria. A maximum force of  $1.01 \times 10^{-4}$  a.u. and the accordingly scaled maximum displacement were adopted as the threshold values for geometry optimization convergence by specifying the internal option Iop(1/7=67). All stationary points were characterized by the eigenvalues of the analytically calculated Hessian matrix.

The Stuttgart 28-electron relativistic effective core potential (ECP28MDF) with accompanying correlation consistent valence triple- $\zeta$  plus polarization (cc-pVTZ-PP) were used for the Ru atom.<sup>52</sup> The g function of this basis set was removed, resulting in a (41s37p25d2f)/[5s5p4d2f]-contracted basis set. The rest of the atoms were treated as follows: All atoms which, at some point in the reaction, are directly bonded (termed a “nearest neighbour”, via a covalent or donor–acceptor bond) to ruthenium and atoms that are bonded to a nearest neighbour with a formal bond order  $\geq 2$  (e.g., the carbon and the oxygen atom of the isocyanate ligand) were treated with a modified version of the correlation consistent valence triple- $\zeta$  plus polarization (cc-pVTZ)<sup>53, 54</sup> basis sets. All other atoms were

treated with the correlation consistent valence double- $\zeta$  plus polarization (cc-pVDZ)<sup>53, 54</sup> basis sets. The cc-pVTZ basis sets were obtained from the EMSL basis set exchange Web site<sup>55</sup> and modified by removing the highest angular momentum function, resulting in the following contractions: C, (18s5p2d)/[4s3p2d]; O, (18s5p2d)/[4s3p2d]; Cl, (41s16p2d)/[5s4p2d]; N (18s5p2d)/[4s3p2d]; S (41s16p2d)/[5s4p2d].

### Single point calculations

The reported energies were obtained through single point calculations on optimized geometries using the gradient corrected PBE<sup>56, 57</sup> functional with the empirical D3 version of Grimme’s dispersion with Becke-Johnson damping<sup>58</sup>, termed PBE-D3(BJ), as implemented in Gaussian 09.<sup>43</sup> The PBE-D3(BJ) functional was chosen due to the excellent performance of the counterpoise-corrected PBE-D3(BJ) functional in reproducing experimental gas-phase relative energies of ruthenium-mediated olefin metathesis.<sup>29</sup> Counterpoise corrections are not included in the present study. However, the much larger basis sets used here (see below) compared to those of the validation study<sup>29</sup> suggest that relative energies of the present work are only negligibly affected by basis set superposition errors (BSSEs).

Numerical integrations were performed using the “ultrafine” grid of Gaussian 09. The SCF convergence criterion was set to  $10^{-5}$ .

The Stuttgart 28-electron relativistic effective core potential (ECP28MDF) with accompanying correlation consistent valence quadruple- $\zeta$  plus polarization (cc-pVQZ-PP) were used for the Ru atom<sup>52</sup>. The C and H atoms were treated with the correlation consistent valence quadruple- $\zeta$  basis set plus polarization (cc-pVQZ)<sup>53, 54</sup> obtained from the EMSL basis set exchange Web site. All other atoms were treated with an extended cc-pVQZ basis set obtained by adding diffuse functions from the “aug-cc-pVQZ Diffuse” set<sup>54, 63</sup> resulting in the following contractions for the modified basis sets: O, (22s7p4d3f2g)/[6s5p4d3f2g]; Cl, (43s20p4d3f2g)/[7s6p4d3f2g]; N, (22s7p4d3f2g)/[6s5p4d3f2g]; S, (43s20p4d3f2g)/[7s6p4d3f2g].

Electrostatic and non-electrostatic (by including the “Dis”, “Rep”, and “Cav” keywords; see the Supporting Information for a sample input file) solvent effects have been estimated within the polarizable continuum solvation model PCM<sup>64–67</sup> using tetrahydrofuran and dichloromethane as solvents. The united atom topological model with atomic radii optimized for Hartree-Fock level of theory (termed “UAHF”) was used for the solute cavity. Finally, a standard state corresponding to 1M infinitely diluted solution and a temperature of 298.15 K has been adopted in the calculation of Gibbs free energies.

It has recently been suggested that DFT-D methods tend to overestimate dispersive interactions.<sup>59</sup> Apparent overestimation of these attractive interactions may arise from lacking or imbalanced treatment of solvent effects,<sup>60–62</sup> from BSSE resulting from incomplete basis sets,<sup>62</sup> or from an unfortunate choice of functional.<sup>62</sup> The density functional used in the

current single-point calculations, PBE-D3(BJ), was selected due to its excellent agreement with experimental relative energies of gas-phase intermediates of ruthenium-based olefin metathesis,<sup>29</sup> and this functional is here used in combination with large, correlation-consistent basis sets that should lead to only negligible BSSE. Finally, both electrostatic and non-electrostatic solvent effects are accounted for. In particular, the solvent model includes solvent–solute dispersion interactions that counterbalance the (otherwise overestimated) intramolecular dispersion. In conclusion, the present computational model is selected with care and is not, for example, expected to lead to apparent overestimation of intramolecular dispersion.

## Experimental

### General procedures

The synthesis of complex **5a** and some of the catalytic tests (e.g., the reactions displayed in Tables 3 and 8) were performed under dry argon atmosphere, either inside a glovebox or using Schlenk techniques, while all the other catalytic reactions were performed in air using ordinary glassware.

Ethanol and isopropanol were purchased from Kemetyl Norge AS, while the other solvents were obtained from Sigma Aldrich.

Hoveyda-Grubbs second-generation catalyst (**3**), silver cyanate, 2,4,6-triphenylbenzenethiol, 1,3,5-tri-tert-butylbenzene, ethyl acetate, and dichloromethane-*d*<sub>2</sub> were purchased from Sigma-Aldrich and used as received. Chloroform-*d* was purchased from Sigma-Aldrich, dried under CaH<sub>2</sub> and distilled prior use. Phenylphosphoric acid was purchased from TCI and used as received. Bis(isocyanato)-(1,3-dimesityl-4,5-dihydroimidazol-2-ylidene)-2-isopropoxybenzylidene)-ruthenium (**5**), and (2,4,6-triphenylbenzenethiolate)-(Cl)-(1,3-dimesityl-4,5-dihydroimidazol-2-ylidene)-2-isopropoxybenzylidene)-ruthenium (**3a**) were prepared according literature procedures.<sup>8, 26</sup>

The olefinic substrates (1-octene, allylbenzene, allyl trimethylsilane, 4-phenyl-1-butene, *N*-allylaniline, 2-(allyloxy)-ethanol, and methyl undecenoate were purchased from Sigma-Aldrich and used as received. For selected catalytic tests allylbenzene (Tables 3 and 8) and 1-octene (Table 3) were degassed before use.

Tetrahydrofuran (THF) and dichloromethane used in the preparation of **5a** and the THF employed in Table 3 were dried and degassed using an MBraun solvent purification system (“Grubbs’ column”), while dry pentane used for the recrystallization of complex **5a** was purchased from Sigma-Aldrich and used as received. CDCl<sub>3</sub> was purchased from Sigma-Aldrich, dried over CaH<sub>2</sub> and distilled before use. Anhydrous CD<sub>2</sub>Cl<sub>2</sub> was purchased from Sigma-Aldrich and used as received.

Potassium 2,4,6-triphenylbenzenethiolate was prepared using a procedure slightly modified from that previously reported from our group.<sup>8, 15</sup> In a glovebox, KH (3.10 mmol)

was added in small portions to a stirred solution of 2,4,6-triphenylbenzenethiol (2.95 mmol) in THF (10 mL). The mixture was stirred at room temperature for 24 hours. The product, a white solid, was isolated by cannula filtration outside the glovebox using a Schlenk line, then washed twice with THF (7 mL) at room temperature, and finally dried inside the glove box (83 % of yield). The quality of the product was evaluated by <sup>1</sup>H-NMR spectroscopy, which showed the disappearance, or only traces, of the thiol proton peak at 3.46 ppm (CDCl<sub>3</sub>).

NMR spectra were recorded on a Bruker Biospin AV600 spectrometer. The chemical shifts are reported relative to the residual solvent peaks.

HRMS (ESI<sup>+</sup>) analysis was recorded by means of a JMS-T100LC AccuTOF<sup>TM</sup> from JEOL, USA, Inc. (Peabody, MA, USA). (Orthogonal accelerated time of flight single stage reflectron mass analyzer and a dual micro channel plate (MCP) detector).

The ATR-IR spectrum of compound **5a** was recorded on a Thermo Nicolet 380 FTIR spectrometer.

The AccuTOF<sup>TM</sup> mass spectrometer was operated with an orthogonal electrospray ionization source (ESI), an orthogonal accelerated time of flight (TOF) single stage reflectron mass analyzer and a dual micro channel plate (MCP) detector.

X-ray diffraction measurements were performed on a Bruker Apex Ultra TXS, rotating anode, CCD instrument doing 0.3–0.5 degree  $\omega$  scans over 182° in four orthogonal  $\phi$ -settings. The samples were cooled using a N<sub>2</sub> blower, series 700 from Oxford Cryosystem. Apart from geometrical corrections, numerical absorption correction by face indexing with Gaussian quadrature integration, and semi-empirical incident beam correction were applied.

Elemental analyses were performed using an Elementar Vario EL III analyzer.

### Preparation of complex **5a**.

In a glovebox, bis(isocyanato)-(1,3-dimesityl-4,5-dihydroimidazol-2-ylidene)-2-isopropoxybenzylidene)-ruthenium **4** (440 mg, 0.67 mmol), and potassium 2,4,6-triphenylthiophenolate (265 mg, 0.70 mmol) were transferred to a 50 mL Schlenk flask, followed by addition of 10 mL of THF, and the mixture was stirred at room temperature for 24 hours. <sup>1</sup>H NMR analysis of the reaction mixture revealed the presence of about 0.2 % of the starting material **4** (estimated by integration of the singlet at 4.16 ppm (CDCl<sub>3</sub>) corresponding to the four hydrogen atoms of the C–C backbone of the imidazoline moiety of the *N,N'*-bis-(mesityl)-4,5-dihydroimidazol-2-ylidene (SImes). The mixture was filtered through celite using THF as solvent, followed by removal of the solvent *in vacuo*. To the residual, potassium 2,4,6-triphenylthiophenolate (13 mg, 0.034 mmol) and 5 mL of THF were added, and the mixture was stirred at room temperature for another 24 hours. <sup>1</sup>H NMR analysis of the reaction mixture showed complete conversion of the starting material **4** to the target product **5a**. The mixture was first filtrated through celite using THF as solvent, followed by removal of the solvent *in vacuo*. The residual was redissolved in 3 mL CH<sub>2</sub>Cl<sub>2</sub>, and then

pentane (40 ml) was slowly added, in such a way as to obtain two separate layers, which were allowed to diffuse slowly (one week) into each other at  $-32^{\circ}\text{C}$ . The grown crystals of **5a**·CH<sub>2</sub>Cl<sub>2</sub> (622 mg, yield 91 %) were then collected, washed three times with pentane, and dried in argon atmosphere. A suitable crystal was selected for X-ray diffraction analysis. The molecule of solvent (CH<sub>2</sub>Cl<sub>2</sub>) present in the crystal lattice is slowly lost with time. <sup>1</sup>H NMR (600.17 MHz, CD<sub>2</sub>Cl<sub>2</sub>):  $\delta$  = 14.32 (s, 1H), 7.73-7.47 (m, 5H), 7.44-7.39 (m, 2H), 7.37-7.29 (m, 3H), 7.26-7.21 (m, 1H), 7.15 (s, br., 1H), 6.99 (t, br, J = 6.9 Hz, 1H), 6.95 (s, br, 2H), 6.89-6.64 (m, 8H), 6.56-6.48 (m, 2H), 4.23 (sept, J = 6.1 Hz, 1H), 3.92 (s, br, 4H), 2.36 (s, 6H), 2.33 (s, 6H), 2.13 (s, 6H), 0.84 (d, J = 6.1 Hz, 3H), 0.53 (d, J = 6.1 Hz, 3H). <sup>13</sup>C<sup>1</sup>H NMR (150.91 MHz, CD<sub>2</sub>Cl<sub>2</sub>):  $\delta$  = 276.88, 276.83, 209.50, 153.80, 149.33, 147.33, 145.55, 145.27, 142.34, 141.54, 140.99, 138.47, 138.37, 138.28, 137.04, 136.13, 131.33, 131.20, 129.55, 129.13, 129.07, 128.95, 128.50, 128.34, 128.17, 127.84, 127.69, 127.24, 126.93, 125.69, 122.82, 121.95, 113.04, 76.23, 51.85, 21.18, 20.90, 20.59, 19.03, 18.68. IR (ATR mode, cm<sup>-1</sup>): 2218 (m,  $\nu(\text{NCO})$ ). HRMS (ESI<sup>+</sup>), *m/z*: 955.29851 [M+Na]<sup>+</sup>; calculated for C<sub>56</sub>H<sub>55</sub>N<sub>3</sub>NaO<sub>2</sub><sup>99</sup>RuS: 955.29721. Elemental analysis, calculated for C<sub>56</sub>H<sub>55</sub>N<sub>3</sub>O<sub>2</sub>SRu·0.5CH<sub>2</sub>Cl<sub>2</sub>: C, 69.41, H, 5.77, N, 4.30; found: C, 69.46, H, 5.75, N, 4.20.

## Acknowledgements

The Norwegian Research Council is gratefully acknowledged for financial support via the FORNY (grant no. 208335) and GASSMAKS (grant no. 203379) programs, as well as for CPU resources granted via the NOTUR supercomputing program. Dr. Bjarte Holmelid is thanked for assistance with the HRMS (ESI<sup>+</sup>) analyses.

## Notes and references

<sup>a</sup> Department of Chemistry, University of Bergen, Allégaten 41, 5007 Bergen, Norway.

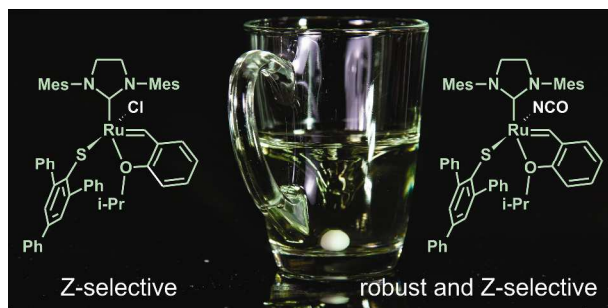
<sup>†</sup> Only in the experiment with **5a** in air a signal at 13.61 ppm, which could belong to the bis-thiolate complex, was detected after one week. The integral of this signal was about one fourth of that of **5**.

<sup>††</sup> Of course, any decomposition pathway requiring the loss of chloride or isocyanate (e.g., degradation of the alkylidene with oxygen)<sup>68</sup> could in principle promote the formation of **3** and **5**.

Electronic Supplementary Information (ESI) available: NMR and HRMS (ESI<sup>+</sup>) spectra, crystallographic data and the CIF file for **5a** with the CCDC reference code 985860. NMR studies of the decomposition of **3a** and **5a** in air and in presence of phenylphosphoric acid. Experimental details of the catalytic tests. Calculated energies and Cartesian coordinates of the optimized structures. See DOI: 10.1039/b000000x/

## References

## Graphical abstract



A tight interplay between theory and experiment has led to the development of a new, highly Z-selective ruthenium-based olefin metathesis catalyst that can be used in air, with unpurified and non-degassed substrates and solvents, and in the presence of acids

- A. Fürstner, *Science*, 2013, **341**, 1357-1364.
- S. Kress and S. Blechert, *Chem. Soc. Rev.*, 2012, **41**, 4389-4408.
- A. J. Jiang, Y. Zhao, R. R. Schrock and A. H. Hoveyda, *J. Am. Chem. Soc.*, 2009, **131**, 16630-16631.
- D. V. Peryshkov, R. R. Schrock, M. K. Takase, P. Mueller and A. H. Hoveyda, *J. Am. Chem. Soc.*, 2011, **133**, 20754-20757.
- C. Wang, F. Haeffner, R. R. Schrock and A. H. Hoveyda, *Angew. Chem. Int. Ed.*, 2013, **52**, 1939-1943.
- K. Endo and R. H. Grubbs, *J. Am. Chem. Soc.*, 2011, **133**, 8525-8527.
- B. K. Keitz, K. Endo, P. R. Patel, M. B. Herbert and R. H. Grubbs, *J. Am. Chem. Soc.*, 2013, **135**, 3300-3300.
- G. Occhipinti, F. R. Hansen, K. W. Törnroos and V. R. Jensen, *J. Am. Chem. Soc.*, 2013, **135**, 3331-3334.
- C. Wang, M. Yu, A. F. Kyle, P. Jakubec, D. J. Dixon, R. R. Schrock and A. H. Hoveyda, *Chem.-Eur. J.*, 2013, **19**, 2726-2740.
- M. B. Herbert, V. M. Marx, R. L. Pederson and R. H. Grubbs, *Angew. Chem. Int. Ed.*, 2013, **52**, 310-314.
- B. L. Quigley and R. H. Grubbs, *Chem. Sci.*, 2014, **5**, 501-506.
- T. J. Mann, A. W. H. Speed, R. R. Schrock and A. H. Hoveyda, *Angew. Chem. Int. Ed.*, 2013, **52**, 8395-8400.
- M. J. Koh, R. K. M. Khan, S. Torker and A. H. Hoveyda, *Angew. Chem.*, 2014, **126**, 1999-2003.
- R. K. M. Khan, S. Torker and A. H. Hoveyda, *J. Am. Chem. Soc.*, 2013, **135**, 10258-10261.
- V. R. Jensen, G. Occhipinti and F. Hansen *Novel Olefin Metathesis Catalysts. Int. Patent Appl. WO 2012032131*, 2012.
- D. Bourgeois, A. Pancrazi, S. P. Nolan and J. Prunet, *J. Organomet. Chem.*, 2002, **643**, 247-252.
- S. H. Hong, D. P. Sanders, C. W. Lee and R. H. Grubbs, *J. Am. Chem. Soc.*, 2005, **127**, 17160-17161.
- F. C. Courchay, J. C. Sworen, I. Ghiviriga, K. A. Abboud and K. B. Wagener, *Organometallics*, 2006, **25**, 6074-6086.
- N. Gimeno, P. Formentin, J. H. G. Steinke and R. Vilar, *Eur. J. Org. Chem.*, 2007, 918-924.
- K. Tanaka, V. P. W. Boehm, D. Chadwick, M. Roepert and D. C. Braddock, *Organometallics*, 2006, **25**, 5696-5698.
- J. Wappel, C. A. Urbina-Blanco, M. Abbas, J. H. Albering, R. Saf, S. P. Nolan and C. Slugovc, *Beilstein J. Org. Chem.*, 2010, **6**, 1091-1098.
- M. Zirngast, E. Pump, A. Leitgeb, J. H. Albering and C. Slugovc, *Chem. Commun.*, 2011, **47**, 2261-2263.
- O. Songis, A. M. Z. Slawin and C. S. J. Cazin, *Chem. Commun.*, 2012, **48**, 1266-1268.
- L. Falivene, A. Poater, C. S. J. Cazin, C. Slugovc and L. Cavallo, *Dalton Trans.*, 2013, **42**, 7312-7317.
- S. Jung, K. Ilg, C. D. Brandt, J. Wolf and H. Werner, *Eur. J. Inorg. Chem.*, 2004, 469-480.
- P. S. Kumar, K. Wurst and M. R. Buchmeiser, *Chem. Asian J.*, 2009, **4**, 1275-1283.
- S. Monfette, J. Marleau-Gillette, J. C. Conrad, R. McDonald and D. E. Fogg, *Dalton Trans.*, 2012, **41**, 14476-14479.
- Y. Minenkov, G. Occhipinti, W. Heyndrickx and V. R. Jensen, *Eur. J. Inorg. Chem.*, 2012, 1507-1516.
- Y. Minenkov, G. Occhipinti and V. R. Jensen, *Organometallics*, 2013, **32**, 2099-2111.
- G. S. Hammond, *J. Am. Chem. Soc.*, 1955, **77**, 334-338.
- N. Bahri-Laleh, R. Credendino and L. Cavallo, *Beilstein J. Org. Chem.*, 2011, **7**, 40-45.
- P. Liu, X. Xu, X. Dong, B. K. Keitz, M. B. Herbert, R. H. Grubbs and K. N. Houk, *J. Am. Chem. Soc.*, 2012, **134**, 1464-1467.
- Y. Dang, Z.-X. Wang and X. Wang, *Organometallics*, 2012, **31**, 7222-7234.
- Y. Dang, Z.-X. Wang and X. Wang, *Organometallics*, 2012, **31**, 8654-8657.
- S. E. Lehman, J. E. Schwendeman, P. M. O'Donnell and K. B. Wagener, *Inorg. Chim. Acta*, 2003, **345**, 190-198.
- T. J. Donohoe, T. J. C. O'Riordan and C. P. Rosa, *Angew. Chem. Int. Ed.*, 2009, **48**, 1014-1017.
- A. Poater and L. Cavallo, *J. Mol. Catal. A-Chem.*, 2010, **324**, 75-79.
- J. S. Kingsbury, J. P. A. Harrity, P. J. Bonitatebus and A. H. Hoveyda, *J. Am. Chem. Soc.*, 1999, **121**, 791-799.
- M. L. Macnaughtan, J. B. Gary, D. L. Gerlach, M. J. A. Johnson and J. W. Kampf, *Organometallics*, 2009, **28**, 2880-2887.
- K. Vehlou, S. Maechling, K. Koehler and S. Blechert, *Tetrahedron Lett.*, 2006, **47**, 8617-8620.
- J. C. Conrad, H. H. Parnas, J. L. Snelgrove and D. E. Fogg, *J. Am. Chem. Soc.*, 2005, **127**, 11882-11883.
- R. Gawin and K. Grela, *Eur. J. Inorg. Chem.*, 2012, 1477-1484.
- M. J. Frisch, G. W. Trucks, H. B. Schlegel, G. E. Scuseria, M. A. Robb, J. P. Cheeseman, G. Scalmani, V. Barone, B. Mennucci, G. A. Petersson, H. Nakatsuji, M. Caricato, X. Li, H. P. Hratchian, A. F. Izmaylov, J. Bloino, G. Zheng, J. L. Sonnenberg, M. Hada, M. Ehara, K. Toyota, R. Fukuda, J. Hasegawa, M. Ishida, T. Nakajima, Y. Honda, O. Kitao, H. Nakai, T. Vreven, J. J. A. Montgomery, J. E. Peralta, F. Ogliaro, M. Bearpark, J. J. Heyd, E. Brothers, K. N. Kudin, V. N. Staroverov, R. Kobayashi, J. Normand, K. Raghavachari, A. Rendell, J. C. Burant, S. S. Iyengar, J. Tomasi, M. Cossi, N. Rega, J. M. Millam, M. Klene, J. E. Knox, J. B. Cross, V. Bakken, C. Adamo, J. Jaramillo, R. Gomperts, R. E. Stratmann, O. Yazyev, A. J. Austin, R. Cammi, C. Pomelli, J. W. Ochterski, R. L. Martin, K. Morokuma, V. G. Zakrzewski, G. A. Voth, P. Salvador, J. J. Dannenberg, S. Dapprich, A. D. Daniels, Ö. Farkas, J. B. Foresman, J. V. Ortiz, J. Cioslowski and D. J. Fox, *Gaussian 09 (Revision A.02)* Gaussian, Inc., Wallingford CT, 2009.
- A. D. Becke, *J. Chem. Phys.*, 1997, **107**, 8554-8560.
- J. D. Chai and M. Head-Gordon, *Phys. Chem. Chem. Phys.*, 2008, **10**, 6615-6620.
- Q. Wu and W. T. Yang, *J. Chem. Phys.*, 2002, **116**, 515-524.
- Y. Minenkov, A. Singstad, G. Occhipinti and V. R. Jensen, *Dalton Trans.*, 2012, **41**, 5526-5541.
- Spartan '08* Wavefunction, Inc., Irvine, CA, 2008.
- F. H. Allen, *Acta Crystallogr., Sect. B*, 2002, **58**, 380-388.
- S. B. Garber, J. S. Kingsbury, B. L. Gray and A. H. Hoveyda, *J. Am. Chem. Soc.*, 2000, **122**, 8168-8179.
- T. A. Halgren, *J. Comput. Chem.*, 1996, **17**, 490-519.
- K. A. Peterson, D. Figgen, M. Dolg and H. Stoll, *J. Chem. Phys.*, 2007, **126**.
- T. H. Dunning, *J. Chem. Phys.*, 1989, **90**, 1007-1023.
- D. E. Woon and T. H. Dunning, *J. Chem. Phys.*, 1993, **98**, 1358-1371.
- D. Feller, *J. Comput. Chem.*, 1996, **17**, 1571-1586.
- J. P. Perdew, K. Burke and M. Ernzerhof, *Phys. Rev. Lett.*, 1996, **77**, 3865-3868.
- J. P. Perdew, K. Burke and M. Ernzerhof, *Phys. Rev. Lett.*, 1997, **78**, 1396-1396.
- S. Grimme, S. Ehrlich and L. Goerigk, *J. Comput. Chem.*, 2011, **32**, 1456-1465.
- H. Jacobsen and L. Cavallo, *ChemPhysChem*, 2012, **13**, 562-569.
- L. Yang, C. Adam, G. S. Nichol and S. L. Cockcroft, *Nature Chemistry*, 2013, **5**, 1006-1010.

61. Y. Minenkov, G. Occhipinti and V. R. Jensen, *J. Phys. Chem. A*, 2009, **113**, 11833-11844.
62. S. Grimme, *ChemPhysChem*, 2012, **13**, 1407-1409.
63. R. A. Kendall, T. H. Dunning and R. J. Harrison, *J. Chem. Phys.*, 1992, **96**, 6796-6806.
64. J. Tomasi and M. Persico, *Chem. Rev.*, 1994, **94**, 2027-2094.
65. J. Tomasi, B. Mennucci and R. Cammi, *Chem. Rev.*, 2005, **105**, 2999-3093.
66. M. Cossi, G. Scalmani, N. Rega and V. Barone, *J. Chem. Phys.*, 2002, **117**, 43-54.
67. G. Scalmani and M. J. Frisch, *J. Chem. Phys.*, 2010, **132**, 114110-114115.
68. M. B. Dinger and J. C. Mol, *Eur. J. Inorg. Chem.*, 2003, 2827-2833.